REPORT DOCUMENTATION PAGE

Form Approved
OMB No. 0704-0188

1. REPORT DATE *(DD-MM-YYYY)*	2. REPORT TYPE	3. DATES COVERED *(From - To)*
	Technical Papers	

4. TITLE AND SUBTITLE

please see attached

5a. CONTRACT NUMBER

5b. GRANT NUMBER

5c. PROGRAM ELEMENT NUMBER

6. AUTHOR(S)

5d. PROJECT NUMBER
3058

5e. TASK NUMBER
RF9A

5f. WORK UNIT NUMBER
346055

7. PERFORMING ORGANIZATION NAME(S) AND ADDRESS(ES)

Air Force Research Laboratory (AFMC)
AFRL/PRS
5 Pollux Drive
Edwards AFB CA 93524-7048

8. PERFORMING ORGANIZATION REPORT

9. SPONSORING / MONITORING AGENCY NAME(S) AND ADDRESS(ES)

Air Force Research Laboratory (AFMC)
AFRL/PRS
5 Pollux Drive
Edwards AFB CA 93524-7048

10. SPONSOR/MONITOR'S ACRONYM(S)

11. SPONSOR/MONITOR'S NUMBER(S)
Please see attached

12. DISTRIBUTION / AVAILABILITY STATEMENT

Approved for public release; distribution unlimited.

13. SUPPLEMENTARY NOTES

14. ABSTRACT

15. SUBJECT TERMS

16. SECURITY CLASSIFICATION OF:			17. LIMITATION OF ABSTRACT	18. NUMBER OF PAGES	19a. NAME OF RESPONSIBLE PERSON
a. REPORT	b. ABSTRACT	c. THIS PAGE	A		Leilani Richardson
Unclassified	Unclassified	Unclassified			19b. TELEPHONE NUMBER *(include area code)* (661) 275-5015

3058RF9A

MEMORANDUM FOR PRS (In-House Publication)

FROM: PROI (STINFO)

03 Oct 2001

SUBJECT: Authorization for Release of Technical Information, Control Number: **AFRL-PR-ED-TP-2001-198**
Mark Archambault; Douglas Talley; Oshin Peroomian, "Computational Analysis of a Single-Element, Shear-Coaxial, GH_2/GO_2 Engine"

AIAA 40th Aerospace Sciences Mtg & Exh.
(Reno, NV, 14-17 January 2002) (Deadline: 01 Nov 01) **(Statement A)**

1. This request has been reviewed by the Foreign Disclosure Office for: a.) appropriateness of distribution statement, b.) military/national critical technology, c.) export controls or distribution restrictions, d.) appropriateness for release to a foreign nation, and e.) technical sensitivity and/or economic sensitivity.
Comments:_____

Signature _____ Date _____

2. This request has been reviewed by the Public Affairs Office for: a.) appropriateness for public release and/or b) possible higher headquarters review.
Comments: _____

Signature _____ Date _____

3. This request has been reviewed by the STINFO for: a.) changes if approved as amended, b) appropriateness of references, if applicable; and c.) format and completion of meeting clearance form if required
Comments:_____

Signature _____ Date _____

4. This request has been reviewed by PR for: a.) technical accuracy, b.) appropriateness for audience, c.) appropriateness of distribution statement, d.) technical sensitivity and economic sensitivity, e.) military/ national critical technology, and f.) data rights and patentability
Comments:_____

APPROVED/APPROVED AS AMENDED/DISAPPROVED

_____

PHILIP A. KESSEL Date
Technical Advisor
Space and Missile Propulsion Division

AIAA-2002-1088

COMPUTATIONAL ANALYSIS OF A SINGLE-ELEMENT, SHEAR-COAXIAL, GH_2/GO_2 ENGINE

Mark Archambault* and Douglas Talley†

Air Force Research Laboratory
Propulsion Directorate
Space and Missile Propulsion Division
Edwards AFB, CA 93524

Oshin Peroomian‡

Metacomp Technologies, Inc.
Westlake Village, CA 91361

Abstract

As part of a program to develop a computational methodology to obtain high-fidelity rocket engine flow solutions, computations were performed on a single-element, gas/gas, H_2/O_2 combustion engine. The solutions are compared with previously reported solutions to this problem, showing that the problem can be solved on a finer grid with a second-order accurate scheme, thus providing another level of detail to the flow physics. Additional time-accurate solutions are also presented. Comparisons among a "quasi-steady" solution, averaged time-accurate solution, and experimental data are made and shown that for inherently unsteady flows, a time-accurate solution does as well as or better than a steady solution.

Introduction

A computational and experimental program of research in gas/gas injection has been initiated in support of staged combustion cycle engines such as the H_2/O_2 Integrated Powerhead Demo or a staged combustion hydrocarbon boost engine. The overall objective of this research is to develop a design methodology for gas/gas injectors. By taking the approach of using experimental measurements to anchor state-of-the-art flow codes, we gain confidence in their predictive capabilities. This in turn leads to a more efficient design process which results in significant savings in full-scale development time and costs.

This paper focuses on a computational methodology to efficiently, accurately, and robustly obtain high-fidelity solutions of combusting rocket engine flows to gain a knowledge and understanding of their features. To that end, simulations of a combusting, single-element, shear-coaxial, H_2/O_2 engine were performed to characterize its flowfield and to validate the CFD++ flow solver for this class of problems. Both steady and transient solutions are examined as well as their sensitivity to different turbulence models. Experimental data are shown for comparison to help determine the accuracy of the code.

This class of problems has been previously investigated both experimentally[1,2] and computationally.[2,3,4] The experiments produced data on hydrogen and oxygen mole fractions, mean and RMS velocities, and OH-radical concentration. This problem has since been used as a benchmark for assessing CFD capabilities for designing gas/gas injectors within a rocket combustor environment. Different numerical methods have been employed including a second-order explicit scheme,[4] a first-order, implicit, upwind differencing scheme,[2,4] and a third-order, implicit, upwind differencing scheme.[4] With each of these schemes, however, the grid was rather coarse. Though

---

* Aerospace Engineer
† Mechanical Engineer
‡ Computer Scientist

their solutions compared well with experimental data, the authors reported that for these conditions the rate of solution convergence as well as the ability to reach a well-converged solution were an issue.

In the present study, the authors used a grid with approximately three times the number of grid cells, resolving the domain in the vicinity of the injectors. This approach has revealed structure near the injector not previously reported. Because the flow is inherently unsteady, time-accurate calculations have been performed that provide a level of detail that gets washed out in the steady calculations. These results, along with comparisons with the experimental data will be discussed.

Computational Model

Calculations were performed using the CFD++ flow solver from Metacomp Technologies, Inc.[5,6] The code has the capability to solve the Reynolds-Averaged Navier-Stokes (RANS) equations, the Large Eddy Simulation (LES) equations, or a RANS/LES hybrid set of equations on 3-D structured and unstructured grids. It is a compressible/incompressible flow code with high- and low-speed capability and has both finite-rate and equilibrium chemistry options. Low-speed flows are solved using a preconditioning algorithm. Explicit (Runge-Kutta) and implicit scheme are available for both steady and unsteady flows.

For the present problem, hydrogen gas flows through an annulus surrounding a central core of gaseous oxygen. The gases enter the combustion chamber where they mix in a shear layer and react. The experimental hardware has a converging section at the end of the chamber which terminates at the throat where the gas is expelled to the atmosphere. In the computational setup, however, this section has been omitted for reasons which will be discussed later.

Oxygen was injected into the chamber at a mass flow rate of 0.042 kg/s (0.01 lbm/sec) with an O/F ratio of 4. The chamber pressurewas specified at 1.29 MPa and the inlet temperature at 297K. The injectors are modeled far enough upstream so that a fully-developed turbulent profile has formed by the time the gas enters the chamber. Standard non-reflecting, subsonic boundary conditions were imposed at the outflow boundary, as well as no-slip conditions at solid surfaces and a symmetry condition on the centerline. All the calculations are done by assuming the flow to be axisymmetric, neglecting the effects of a nitrogen purge used in the experiment to cool the optical access.

Computations were run at the ASC Major Shared Resource Center on 16 processors of an SGI Origins 2000 computer. CFD++ was set up to run the two-dimensional, axisymmetric, compressible, real gas equations. They were discretized with a second-order, upwind scheme on a grid consisting of 53740 grid cells. The grid was stretched to resolve the region near the injectors and to provide an adequate number of grid cells within the boundary layer inside the injectors. The steady calculations used a second-order accurate, preconditioned, implicit scheme with upwind differencing while the time-accurate calculations utilized an implicit, second-order dual time stepping algorithm. Submodels included a realizable $k-\varepsilon$ turbulence model[7] and the Anderson 9-species, 19-reaction chemistry mechanism[8] solved with a finite-rate kinetics scheme and constant-pressure combustion model.

Computational Issues

Because of the unsteady nature of the problem, several unexpected computational issues arose. The first of these was how to get the propellants to ignite and continue to combust. Initial attempts focused on obtaining a cold-flow solution, followed by heating to 2500-3500K the short length of wall on the injector face that separates the oxygen tube from the hydrogen annulus. However, this failed to ignite the flow because the injection velocities were too high to allow sufficient heat transfer to the gases in the mixed region to cause ignition.

As an alternative approach, a heat source set to a temperature of 2500K was applied in a box inside the computational domain. This box was located so as to correspond to the location of the propane igniter in the experimental hardware and its size was approximated to the size of the actual igniter flame. While this approach did initiate combustion, it significantly increased the time to convergence due to the increased duration of the start-up transient. Because the igniter was located a few inches downstream of the injectors, once ignited, the flame would propagate upstream along the outer boundary. This set up a situation from which it was difficult to obtain a steady solution because hot combustion products remained in the region above the injectors, upstream in the chamber, and would only slowly flush out.

To eliminate this problem, the downstream heat source was removed and a smaller heat source was placed immediately downstream of the injectors and extended approximately 0.5 inches into the chamber. As in the previous approach, the temperature in this region was set to 2500K. As the cold propellants passed through this region, they were sufficiently heated to ignite. This approach resolved the issues of a backwards propagating flame and of having combustion products located near the upstream outer surface. After several computational runs, it was determined that the solution could be reached without obtaining a prior cold-flow solution and by reducing the heat source temperature to 1500K.

Another issue that arose was attaching the flame to the injector lip and keeping it stable. Initial attempts at a solution showed that the numeric algorithm would cause the flame to lift approximately an inch from the injector tip. Experimental data and previously reported calculations showed that the flame does attach to the lip under these flow conditions. Grid resolution in the injector region was increased in an attempt to get the flame to attach to the lip; however, this exacerbated the problem with the lifting of the flame. The flame sheet would start to fluctuate, become unstable, and ultimately the flame would extinguish.

The solution to this problem proved to be the solution to a third issue that wasn't entirely unexpected. As discussed in reference 4, the rate of convergence for this problem was slow, requiring a large number of iterations to reach a solution. In the present calculations, two factors contributed to the slow convergence. The first, already discussed, arose from igniting a cold-flow solution by way of a heat source far downstream of the injectors. This increased the duration of the start-up transient as the flame propagated upstream. The second contributing factor was a result of using a structured grid. Though the final solutions do not account for the converging section of the nozzle present in the experiment, initial calculations did include this region. As the grid was stretched downstream into the nozzle section, it became excessively fine, causing the solution to advance too slowly. Internal zonal boundaries that would have allowed for a coarser grid within the nozzle were not a feasible solution.*

By removing the converging nozzle section, the rate of convergence in the rest of the chamber (where the solution was of more interest) was increased. Further, the stability issues associated with the flame sheet and having it attach to the injector lip improved. The reason for the improvement is that some preconditioning algorithms have difficulty handling low-speed to high-speed flows in the same calculation. In this problem when the nozzle was present, upstream flow velocities were near zero, especially in the region away from the injectors, and would accelerate to near sonic velocities inside the nozzle.

To further improve the flame stability, the algorithm was modified to allow the pressure, temperature, and species to equilibrate properly at each iteration. By using an underrelaxation technique, the velocity and pressure were able to adjust smoothly to a slower evolving temperature. This treatment, along with removing the nozzle section, stabilized the flame sheet and anchored the flame to the injector lip.

* The code has since been modified so that internal boundary conditions can be applied, eliminating the problem of having an excessively fine grid in the converging section of a combustion chamber.

Results

The first set of calculations were designed to obtain a solution to the steady RANS equations. The CFL number ranged from 1 to 50 during the 6000 iterations run, by which time the solution residual had fallen to approximately 0.01. Though an additional 6000 iterations were performed, the computation did not reduce the residual any further, but only fluctuated about 0.01. The reason the residual could not be driven lower is because the problem itself is physically unsteady. The strong velocity gradient between the injected gases causes the turbulent shear layer to fluctuate. Experimental measurements also suggest a highly unsteady flow.[1] The high residual values indicate that there is no true steady solution to this problem, though it is possible to obtain what one might call a "quasi-steady" solution. This "quasi-steady" solution would be the best solution obtainable from the steady RANS equations, and though it should not be viewed as a quantitative solution, it can be used to discern generalities.

Because previous calculations of this problem were conducted to provide a steady solution, it is prudent at this point to compare the performance of CFD++ with the performance of other codes. Penn State University's flow solver[9] solved this problem on a grid the size of 151 x 101 cells, about 30% of the number of cells used with the CFD++ code. The coarser mesh and a first-order scheme allowed fluctuations to be damped out so that a steady solution could be obtained in approximately 10000 iterations. The numerical scheme used in this code was similar to that used in CFD++ in that it is a preconditioned, coupled, implicit, time-marching algorithm. The code used at DLR, AS3D,[3] used a second-order, explicit, finite volume approach. Because of the explicit nature of the scheme, each iteration was completed in less time than a single iteration in the present implicit scheme; however, due to numerical stability concerns, a low CFL number had to be utilized and more than 100,000 time steps were required. Finally, the FDNS code[10] from NASA Marshall used a pressure-based algorithm. For this problem, a third-order upwind scheme was employed along with an implicit Euler marching approach. While the investigators who used FDNS reported reasonable convergence rates for this problem, they believed that multi-element injectors would cause additional difficulties. All three codes gave comparable results for the "quasi-steady" problem which reasonably match experimental data.[4] Additional studies by all groups would be interesting and useful in providing additional comparisons of the various computational models.

To garner a more accurate understanding of the flow, a second set of calculations were performed to obtain time-accurate solutions. Since the engine start-up transients were not of interest, the starting point for

the unsteady calculations was the "quasi-steady" solution obtained in the first calculation. The solution was advanced in time increments of one microsecond with a total of 24000 time steps performed beyond the "quasi-steady" results. After approximately 6000 steps, the first graphically noticeable disturbances produced in this calculation had exited the computational domain and after 12000 steps, the influence of the initial condition was completely eliminated.

Figure 1 shows contours of OH concentrations which give an indication as to the location of the flame. Figure 1a depicts an instantaneous snapshot of the flow after 2.0 ms. Results of the last 6000 time steps[§] of the unsteady calculations were averaged and are shown in Figure 1b. In Figure 1c, the "quasi-steady" solution is shown. Because it is assumed in the steady RANS model that the flow is steady, solutions of these equations cannot capture the flapping of the flame that is evident in Figure 1a. This leads to an erroneous steady solution as can be seen by comparing Figure 1b with Figure 1c. The time-averaged flame is actually thicker than one is led to believe by the "quasi-steady" results and the gradient in the OH concentration not as steep.

Figure 2 presents a close-up of the injector lip, showing details of the flame attachment for the averaged time-accurate results. Though not shown, the "quasi-steady" results show similar patterns. In Figure 2a, OH concentrations show that the flame is not symmetrically attached on the lip, but rather makes contact with the entire lip and streams off closer to the hydrogen edge. A counterclockwise-rotating recirculation zone is evident in Figure 2b which stabilizes the flame to the lip. The finer grid (compared with previously reported calculations) allowed the flow solver to capture these details.

The hydrogen mole fraction is plotted in Figure 3. The results are compared with experimental data at 1 in., 2 in., and 5 in. downstream of the injector. The hydrogen exits the injector and mixes with the oxygen in a narrow shear layer at r/R_0 = 1.2 to 1.4. The hydrogen diffuses out towards the wall, but not into the oxygen core. At 1 in., the averaged time-accurate results do about as well as the "quasi-steady" results when compared with experiment. At 2 in., the time-accurate results do a slightly better job at predicting the slope of the gradient through the shear layer at r/R_0 = 1.3, though neither results capture the actual gradient in the vicinity of the centerline. This may be an effect caused by the spatial averaging done by the Raman spectroscopy technique used to experimentally measure these profiles where the spatial averaging was done over the size of the probe volume. Averaging the computational data over a similar volume would determine if this were indeed the cause.

Another feature of the data at the most-upstream location is that the mole fraction of the data significantly decreases at the outer edges of the shear layer. This has been previously reported as likely being caused by the nitrogen curtain used in the experiment to cool the optical windows. The nitrogen would mix with the hydrogen and naturally reduce the hydrogen mole fraction. This nitrogen curtain was not accounted for in the computations.

At the third axial station at x = 5 in., the "quasi-steady" results do a better job of predicting the hydrogen mole fraction profile at the outer edges of the shear layer (r/R_0 = 2); however, the profile is again square near the centerline. The time-accurate results predict a much thicker profile at this station, though do better to predict the slope of the profile in the vicinity of the centerline. There are a number of possibilities for the discrepancies between the data and the calculation including the absence of the nozzle, coarsening of the downstream grid, and an improper value for the turbulent Schmidt number (currently set to 0.9). Characteristics of the computational results may be different if any of these factors were changed. This will be investigated in future work.

Figure 4 shows profiles of oxygen mole fraction. Again, the averaged time-accurate results do about as well as the "quasi-steady" results when compared with the experimental data. As with the hydrogen profiles, both sets of computations overpredict the species gradient near the centerline of the chamber at the first two stations, but otherwise match the profile. At x = 5 in., the computational results again do not as accurately predict the flow phenomena and is likely attributable to one of the factors previously mentioned.

The mean axial velocity is plotted in Figure 5. Here, it can be seen that the hydrogen gas exits the injector with a greater velocity than the oxygen, creating the shear layer in the vicinity of r/R_0 = 1.3. The hydrogen rapidly decelerates from a peak of approximately 120 m/s at one inch downstream of the injectors to approximately 60 m/s after five inches. It appears that the unsteady results better agree with the experimental data than do the "quasi-steady" results. At the first two axial stations the "quasi-steady" results significantly over-predict the peak velocities of the hydrogen stream by more than 20%. Both calculations accurately predict the velocity peak of the oxygen stream. Downstream, at x = 5 in., the time-accurate calculation does not match the experimental data. In fact, there still exist signs of the shear layer as evidenced by the dip in the velocity at the centerline. No similar dip is apparent in the data.

[§] Averages of the last 12000 iterations were also performed, to ensure that frequency of major flow structures was high enough to provide an accurate time-averaged solution within 6000 iterations. Because the two averages were essentially identical, it was determined that using only the last 6000 iterations was sufficient.

In Figure 6 it appears that the "quasi-steady" results predict the RMS axial velocity slightly better than the time-accurate results at the velocity peaks, though the time-accurate results are qualitatively correct. The data and the computations show that the gases exit the injectors with a high turbulence intensity and that intensity is significantly attenuated by the time the flow reaches the third axial station. Both calculations under-predict the RMS velocity within the oxygen core at the first two axial stations. The discrepancies may have to do with an inadequate turbulence model. In these calculations, a standard $k-\varepsilon$ model was used, though perhaps a cubic $k-\varepsilon$ or other turbulence model will do a better job. At the last axial station, both calculations seem to well predict the data; however, given the inaccurate predictions of other quantities at this station, the good agreement in the RMS velocity should be attributed to coincidence more than anything else.

Lastly, profiles of temperature are plotted in Figure 7. Though no experimental data is available for comparison, the plots demonstrate how the "quasi-steady" results predict a thinner flame because the solution to the steady RANS equations cannot resolve the flapping of the flame. The temperature peaks at approximately 3400K where the reaction occurs within the shear layer (c.f. Figure 1). The lower temperatures at the center of the oxygen core and the hydrogen annulus represent the cooler inlet temperatures. Far from the injectors where the temperature is between 550K at x = 1 in. to nearly 1000K at x = 5 in., one can see the effects of heat transfer from the flame and from the hot combustion gases. Figure 8 shows that a significant amount of water exists near the walls, at least partially accounting for the higher temperatures in this region.

Summary and Conclusions

Calculations were performed on a single-element, gas/gas, H_2/O_2 combustion engine as part of a program to develop a computational methodology to be used to predict rocket engine flow fields. This problem was chosen to validate the ability of the CFD++ flow code to solve this class of problems. The code was shown to be able to reasonably predict the characteristics of shear mixing layer on a fine grid, capturing details that a coarser grid could not. Additionally, it was shown that the code was able to produce a "quasi-steady" solution with a second-order accurate preconditioned numerical scheme in less time than previously reported computations. This is important in that turn-around times for computations, and thus for the overall design and analysis time, can be reduced.

The results also showed that for this inherently unsteady problem, solutions obtained by way of solving the steady flow equations give (sometimes significantly) different results than an averaged time-accurate solution. In the results presented here, the time-accurate solutions predicted the experimental data as well as or better than the "quasi-steady" solution in most cases. The exception to this would be at the axial station located five inches from the injector, where it seemed the "quasi-steady" results better matched the data. However, this is likely due to the fact that the converging section of the chamber, present in the experiment, had been neglected in the computation to facilitate the convergence rate. Thus, the flow pattern would likely be altered in the simulation from that in the actual engine.

Differences in the overall flame structure were also seen between the two sets of computations. A very thin flame that does not meet at the centerline appeared in the "quasi-steady" solution whereas a much thicker flame was apparent in the averaged-time accurate results. This was due to the fact that the flame fluctuated as it burned, thus increasing the thickness of the averaged flame position. A steady solution can not capture this phenomenon because the steady flow equations have a built-in assumption that there are no fluctuations of the flow quantities within the flow.

References

1. Moser, M. D., Merenich, J. J., Pal, S., & Santoro, R. J., "OH-Radical Imaging and Velocity Field Measurements in a Gaseous Hydrogen/Oxygen Rocket," AIAA 93-2036, 29th AIAA/SAE/ASME/ ASEE Joint Propulsion Conference & Exhibit, Monterey, CA, June 1993.

2. Foust, M. J., Deshpande, M., Pal, S., Ni, T., Merkle, C. L., & Santoro, R. J., "Experimental and Analytical Characterization of a Shear Coaxial Combusting GO_2/GH_2 Flowfield," AIAA 96-0646, AIAA 34th Aerospace Sciences Meeting & Exhibit, Reno, NV, Jan. 1996.

3. Schley, C. –A., Gagemann, G., & Golovitchev, V., "Comparison of High Pressure H_2/O_2 Rocket Model Engine Reference Simulations," AIAA 95-2429, 31st AIAA/ASME/SAE/ASEE Joint Propulsion Conference & Exhibit, San Diego, CA, July 1995.

4. Schley, C. –A., Gagemann, G., Tucker, P. K., Venkateswaran, S., & Merkle, C. L., "Comparison of Computational Codes for Modeling Hydrogen-Oxygen Injectors," AIAA 97-3302, 33rd AIAA/ASME/ SAE/ASEE Joint Propulsion Conference & Exhibit, Seattle, WA, July 1997.

5. Chakravarthy, S., & Peroomian, O., "Some Internal Flow Applications of a Unified-Grid CFD Methodology," AIAA 96-2926, 32nd AIAA/ASME/

SAE/ASEE Joint Propulsion Conference & Exhibit, Lake Buena Vista, FL, July 1996.

6. Peroomian, O., Chakravarthy, S., & Goldberg, U., "A 'Grid-Transparent' Methodology for CFD," AIAA 97-0724, 35th Aerospace Sciences Meeting & Exhibit, Reno, NV, Jan. 1997.

7. Goldberg, U., Peroomian, O., & Chakravarthy, S., "A Wall-Distance-Free $k-\varepsilon$ Model with Enhanced Near-Wall Treatment," *J. of Fluids Engineering*, vol. 120, Sept. 1998, pp. 457-462.

8. Anderson, J. D., *Hypersonic and High Temperature Gas Dynamics*, McGraw-Hill, 1989, Table 13.2.

7. Chen, Y. S., "Compressible and Incompressible Flow Computations with a Pressure Based Method," AIAA 89-0286, 27th AIAA Aerospace Sciences Meeting & Exhibit, Reno, NV, Jan. 1989.

8. Ventakeswaran, S., Weiss, J. M., Merkle, C. L., & Choi, Y. –H., "Propulsion-Related Flowfields Using the Preconditioned Navier-Stokes Equations," AIAA 92-3437, 28th AIAA/SAE/ASME/ASEE Joint Propulsion Conference & Exhibit, Nashville, TN, July 1992.

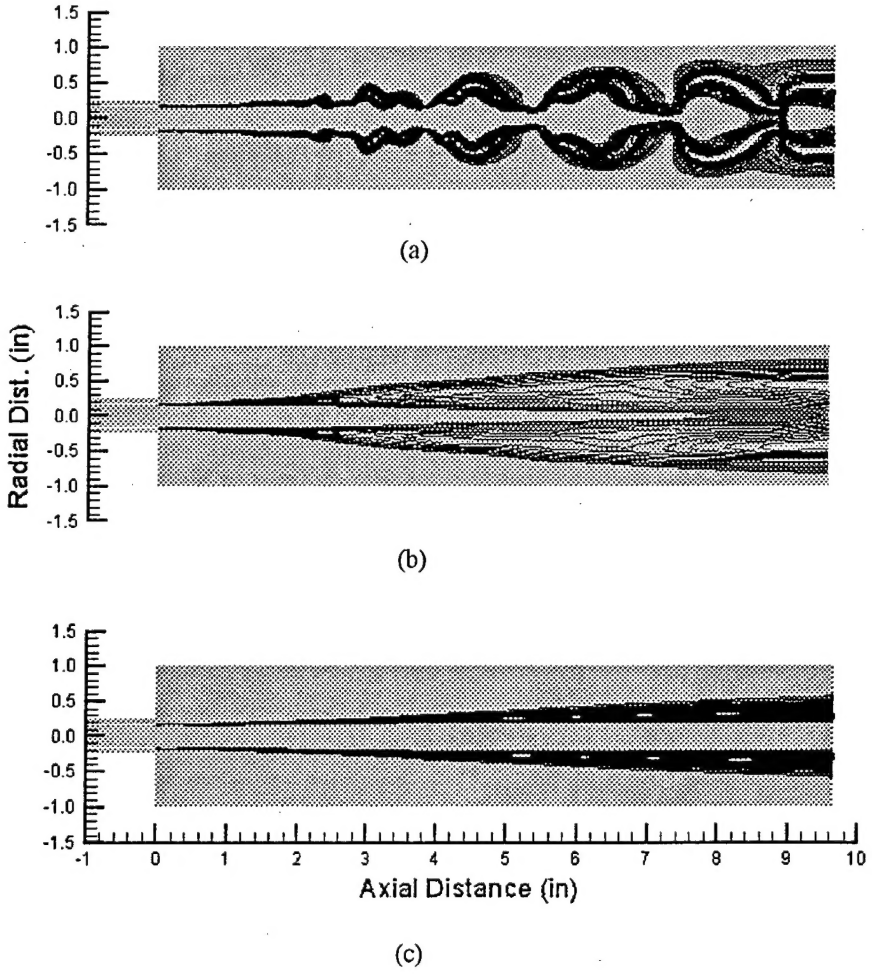

Figure 1. OH concentration contours from (a) instantaneous, (b) averaged time-accurate, and (c) "quasi-steady" solutions.

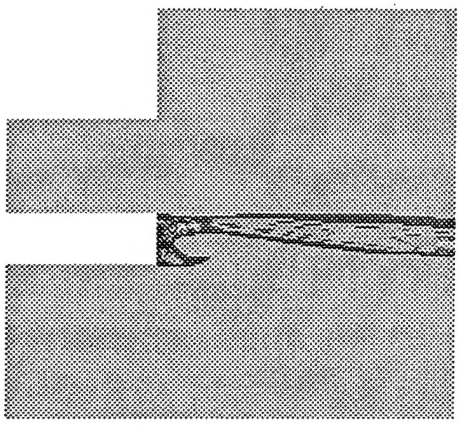

(a)

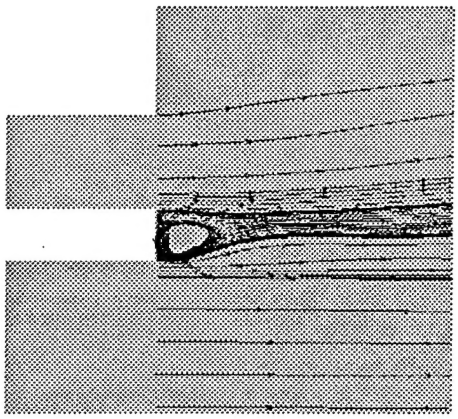

(b)

Figure 2. (a) OH concentration contours and (b) stream traces in the vicinity of the flame attachment point at the lip of the injectors.

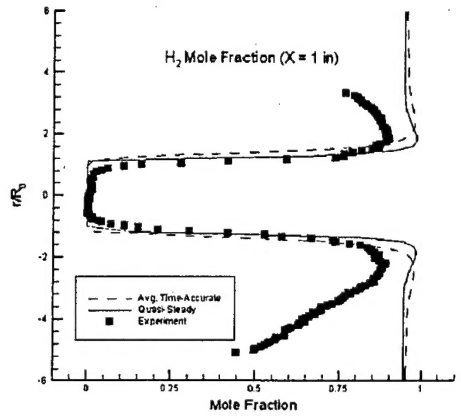

(a)

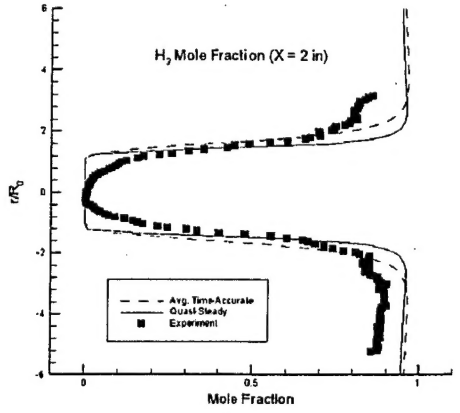

(b)

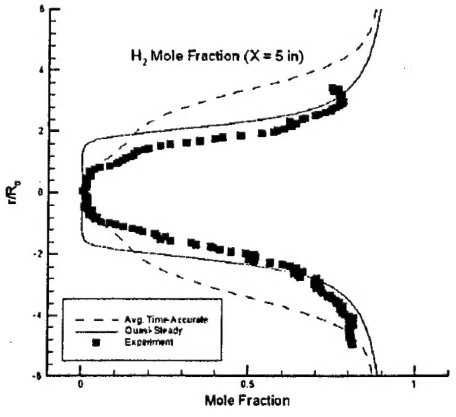

(c)

Figure 3. Hydrogen mole fraction profiles at (a) 1 in., (b) 2 in., and (c) 5 in. downstream of injectors.

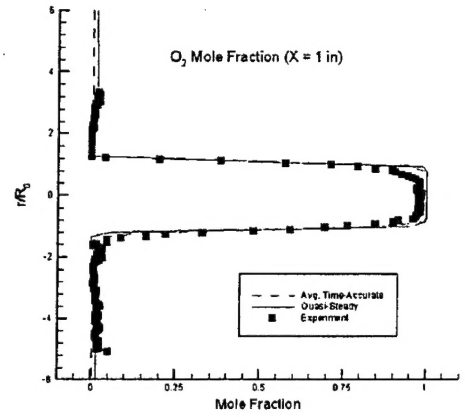

(a)

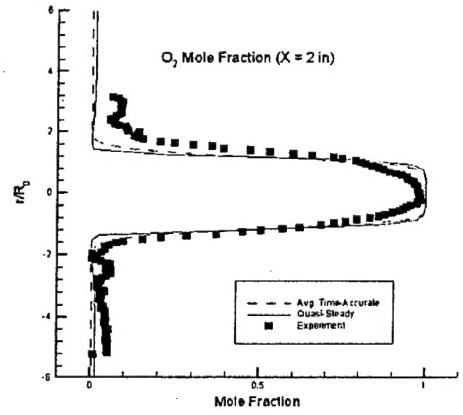

(b)

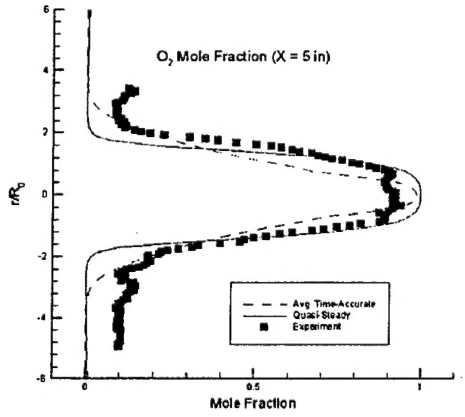

(c)

Figure 4. Oxygen mole fraction profiles at (a) 1 in., (b) 2 in., and (c) 5 in. downstream of injectors.

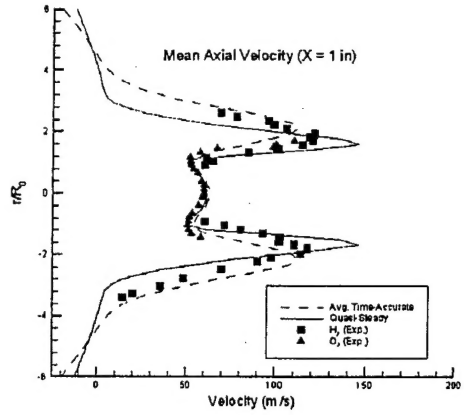

(a)

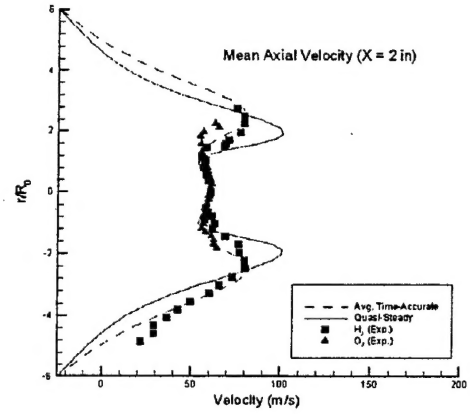

(b)

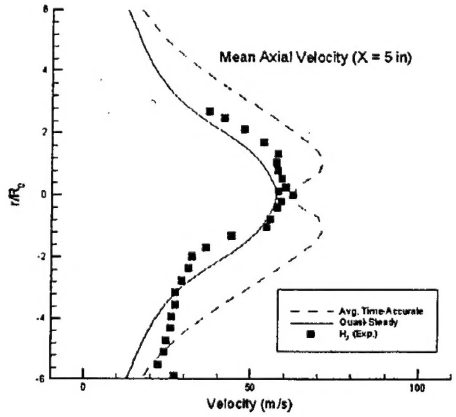

(c)

Figure 5. Mean axial velocity profiles at (a) 1 in., (b) 2 in., and (c) 5 in. downstream of injectors.

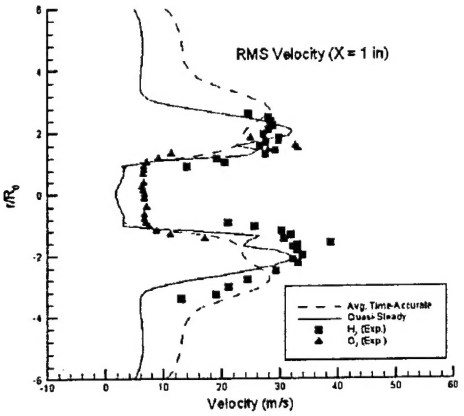

(a)

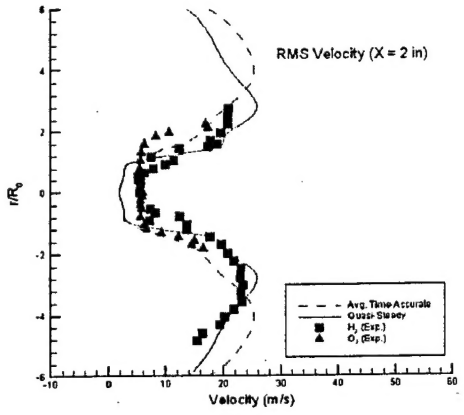

(b)

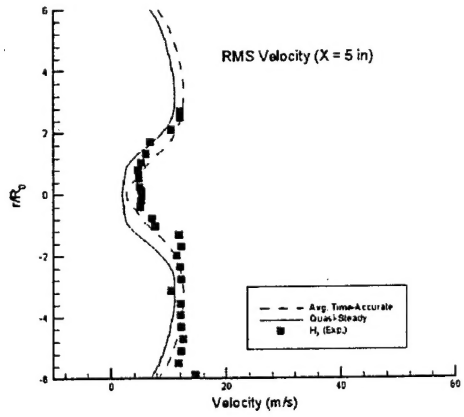

(c)

Figure 6. RMS velocity profiles at (a) 1 in., (b) 2 in., and (c) 5 in. downstream of injectors.

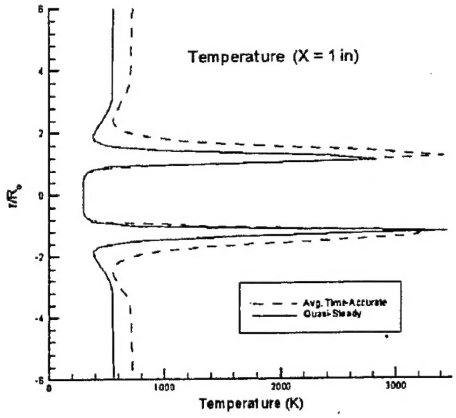

(a)

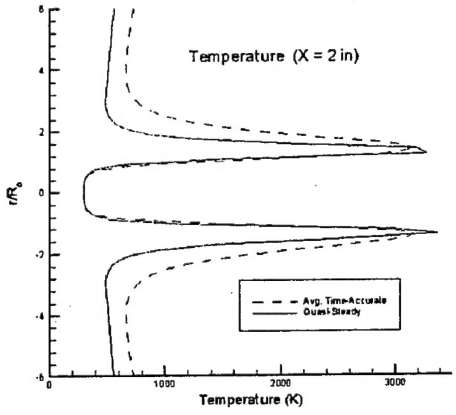

(b)

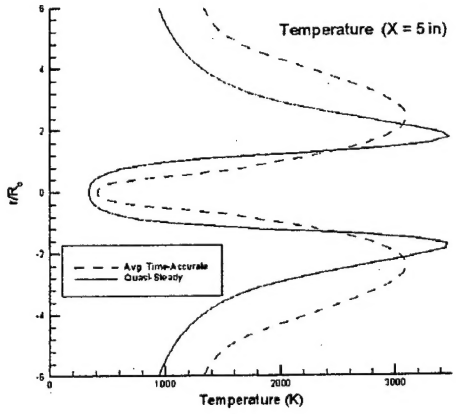

(c)

Figure 7. Temperature profiles at (a) 1 in., (b 2 in., and (c) 5 in. downstream of injectors.

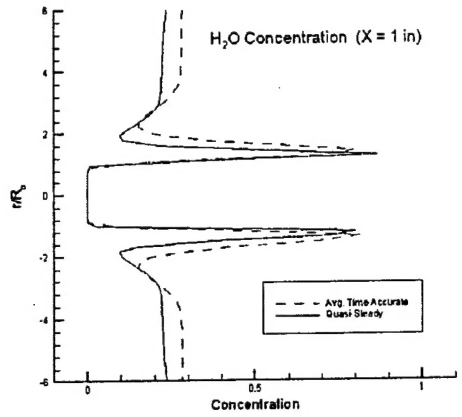

(a)

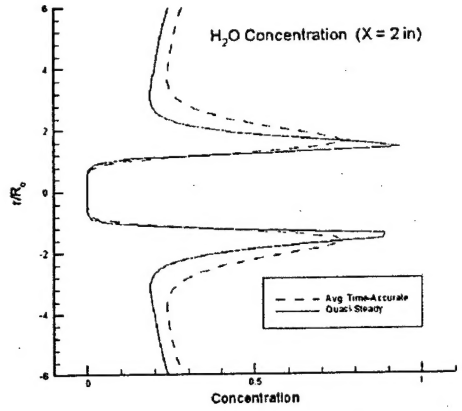

(b)

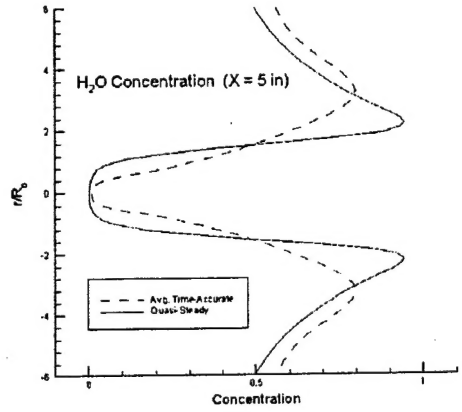

(c)

Figure 8. Water concentration profiles at (a) 1 in., (b) 2 in., and (c) 5 in. downstream of injectors.